# Wireless sensor networks for permanent health monitoring of historic buildings

Daniele Zonta[1]*, Huayong Wu[1], Matteo Pozzi[1], Paolo Zanon[1], Matteo Ceriotti[2], Luca Mottola[3], Gian Pietro Picco[4], Amy L. Murphy[2], Stefan Guna[4] and Michele Corrà[5]

[1]*Department of Mechanical and Structural Engineering, University of Trento, Via Mesiano 77, 38123 Trento, Italy*
[2]*IRST, Bruno Kessler Foundation, Via Sommarive 18, 38123 Trento, Italy*
[3]*Swedish Institute of Computer Science, Isafjordsgatan 22/Kistagången 16, 16440 Kista, Sweden*
[4]*DISI, University of Trento, Via Sommarive 14, 38123, Trento, Italy*
[5]*Tretec S.r.l., Via Solteri 38, 38121 Trento, Italy*

**Abstract.**   This paper describes the application of a wireless sensor network to a 31 meter-tall medieval tower located in the city of Trento, Italy. The effort is motivated by preservation of the integrity of a set of frescoes decorating the room on the second floor, representing one of most important International Gothic artworks in Europe. The specific application demanded development of customized hardware and software. The wireless module selected as the core platform allows reliable wireless communication at low cost with a long service life. Sensors include accelerometers, deformation gauges, and thermometers. A multi-hop data collection protocol was applied in the software to improve the system's flexibility and scalability. The system has been operating since September 2008, and in recent months the data loss ratio was estimated as less than 0.01%. The data acquired so far are in agreement with the prediction resulting a priori from the 3-dimensional FEM. Based on these data a Bayesian updating procedure is employed to real-time estimate the probability of abnormal condition states. This first period of operation demonstrated the stability and reliability of the system, and its ability to recognize any possible occurrence of abnormal conditions that could jeopardize the integrity of the frescos.

## 1. Introduction

As suggested by Farrar and Worden (2007), structural health monitoring refers to technologies used to assess the integrity of structures, to detect damage early and before reaching the limit state, and to periodically or continuously provide information to help reach efficient and cost effective maintenance decisions. In general, this concept applies to aerospace, mechanical and civil engineering structures. It is likewise clear that there are major differences between monitoring an historic structure and an aircraft or a bridge. Many historic buildings, well beyond their original design life span, are still preserved and used because of their historical status, artistic value or structural importance. With the accumulation of degradation and deterioration, an assessment of the structural

---

*Corresponding Author, Assistant Professor, E-mail: daniele.zonta@unitn.it

integrity and safety becomes increasingly important, and an automated and effective damage diagnostic system is very useful. Examples of monitoring of historic structures can be found in the literature, while more and more conferences on historic buildings dedicate special sessions to this topic (D'Ayala and Fodde 2008, Modena *et al.* 2004).

A monitoring system includes a certain number of distributed sensors which are responsible for collecting measurements from different positions, and a central data acquisition system that is responsible for storing all the data from different sensors for further processing and analysis. Today, most sensor systems are cable-based and employ hub-spoke connection, with tens or even hundreds of remote sensors wired directly to a centralized data acquisition hub.

The potential advantages of wireless sensor technologies and wireless sensor networks (WSN) over conventional cabled monitoring systems have been repeatedly remarked in the literature (Lynch *et al.* 2002a, Spencer *et al.* 2003, Kijewski-Correa *et al.* 2005, Lynch and Loh 2006): low installation cost, highly scalable features, remote tasking ability and low-level invasion of host structures. In modern structures, wireless sensors are usually motivated by economics: Lynch and Loh (2006) have noted that the high installation and maintenance cost of cable-based sensors, is a significant impediment to their use for structural monitoring. Conversely, ease of deployment, absence of cables and limited visual impact of the system are a key asset in monitoring heritage buildings, especially in buildings containing works of art. WSNs can meet these needs, of reduced invasiveness, even with large numbers of sensors, also offering flexible sensor system configurations.

A wireless sensor (usually called sensor node in a WSN) is an updated version of the traditional sensor, operating as an autonomous data acquisition node with wireless communication (Lynch and Loh 2006). Moreover, wireless sensors can play a greater role in processing monitored data by moving the intelligence closer to the measurement point (Lewis 2004), which turns the pure data acquiring sensors into intelligent nodes and makes the wireless sensor network more powerful and energy efficient.

Many products are now commercially available for integration in WSNs for structural health monitoring. A number of authors (see for instance Xu *et al.* 2004, Kijewski-Correa *et al.* 2005), have noted that initial WSN attempts were wireless data acquisition systems emulating the hub-spoke architecture in a traditional monitoring system, replacing cables from sensors to hub with wireless communication. In other cases, the original cabled data transmission from field to server was replaced by various wireless communication technologies. Pines and Lovell (1998) proposed a conceptual framework for a remote wireless health monitoring system for large civil structures using spread spectrum wireless modems, with a range of 3 to 5 miles and data rates greater than 28.8 kbps. In the system all the data, collected by a ruggedized data acquisition system near the structures, could be downloaded via the wireless modems. Arms *et al.* (2008) also reported some early applications of remote monitoring technologies using the mobile phone network from the structure to the base station. However, in the local network, the sensors are wired to the local data acquisition system.

All these applications differ from intelligent WSN with local computational capabilities, therefore they are merely an exercise in the use of wireless communication for structural health monitoring. Moreover, replacing cables from site to server in a traditional system with wireless does not create a WSN, and the critical issues due to long cables from sensors to hub are still not removed. Also, with the increasing number of wireless nodes in a network, the simple hub-spoke model will suffer problems due to low bandwidth and limited power supply; in a wireless sensor network the scarcest resource is power.

Limited power is still an obstacle, limiting network lifetime and preventing widespread use of

WSN for permanent building monitoring. This is especially true in the case of historic buildings, where the typical problems (subsidence, cracks, tilting, etc.) normally require years or even decades of observation of the structure behavior.

One of the most energy consuming operations in a WSN is data transmission (Lewis 2004). Therefore, the traditional hub-spoke architecture with only single hop strategy in each transmission path is apparently not energy efficient for monitoring applications. To overcome this, computation power is deployed at the sensor node to process the raw data, minimizing data transmission over the network. Moreover, since the power demand in wireless transmission increases with the square of the distance between source and receiver (Lewis 2004), multi-hop short data transmission requires less energy than a single long hop, for the same overall transmission distance, and this can extend the service life and flexibility of the network.

To deploy computation power at a sensor node and hence allow a distributed architecture in structural health monitoring, a number of engineering analysis procedures have been enabled at the nodes. This requires use of an appropriately selected core module. In development of wireless sensing units, Lynch *et al.* (2002b) paid much attention to selecting adequate core hardware, responsible not only for data collection from on-board sensing transducers, but also used for data cleansing and processing. In their paper an accelerometer wireless sensor node was designed and tested using an enhanced Atmel RISC microcontroller, available on the market, to accommodate the local data processing algorithm. Sazonov *et al.* (2004) also presented an intelligent sensor node for continuous structural health monitoring, where an ultra-low power microcontroller (MSP430F1611 from Texas Instruments) was adopted for local computing. On the other hand, special attention was paid to integrating the structural health monitoring algorithm, with data compression, system identification and damage detection, into the wireless sensor network. Caffrey *et al.* (2004) developed a Wisden system based on a Mica2 "mote" for structural health monitoring applications, with a damage detection algorithm. In this scheme a simple network architecture was adopted with a single central base station responsible for storing and processing all the measurements. Differing from this centralized processing scheme, Clayton *et al*. (2006) proposed a decentralized data processing network architecture to exploit the local computational abilities on each node. At each sensor, the data will be first locally processed by implementing a damage localization algorithm to reduce the burden of data transmission. For more information on this aspect, see the summary review by Lynch and Loh (2006).

In response to the limited power in a network, a multi hop wireless network (Caffrey *et al*. 2004, Kurata *et al.* 2005) is a good way to avoid long distance data transmission. To improve damage detection reliability and overall effectiveness of the sensor network, Kijewski-Correa *et al.* (2005) designed a multi-scale wireless sensor network fusing the data from distributed and heterogeneous sensor nodes for a more robust and effective approach to decentralized damage detection.

However, most off-the-shelf wireless platforms or hardware devices are not produced specifically for civil engineering applications, even less for the specific needs of the architectural heritage. Unnecessary integration of components in a wireless node increases the cost and power consumption, hardly satisfying the requirements of structural health monitoring. The relatively high cost and limited life of the sensor nodes are major obstacles to the use of wireless sensor technology in real projects, especially for long term applications (Straser and Kiremidjian 1998, Bennett *et al*. 1999, Kim *et al*. 2007).

This paper introduces the development of a dedicated WSN and its application to an historic building, the medieval Torre Aquila in the City of Trento, Italy. A brief description of the monument is

given in the next Section, along with the reasons for installation of a permanent system and for the choice of WSN as a technology. In Section 3, we introduce the customized hardware and dedicated software developed for our specific requirements, and present the installation of the whole wireless sensor system. The system has been operating since September 2008. In Section 4, a summary of the data acquired to date is presented, and the long term reliability and stability of the system is discussed; in the same section, we also explain with some examples how the raw data are processed in order to provide the owner with information on the state of stability of tower. Finally, some concluding remarks are given at the end of paper.

## 2. Description of Torre Aquila

The Aquila Tower, a part of Buonconsiglio Castle, is a 31 m tall medieval tower located in the city of Trento. As reported in Castelnuovo (1987), the original construction probably dates back to the 13th century: at that time it was a simple defence tower, part of the city wall, above the city gate that was intended for the guard. At the end of the 14th century, the tower was radically modified by prince-bishop George of Liechtenstein, who intended to create a private apartment for his personal use. At the time, the tower was extended, elevated, finely decorated, and directly connected to the bishop's residence, the nearby Buonconsiglio Castle; what we see today is the result of this alteration (Fig. 1). The building is rectangular in plan, 7.8 m by 9.0 m, and features five floors, including the ground level, a passage covered by a barrel vault.

Although the tower appears to be nearly symmetrical in shape, we expect it to show strongly asymmetrical mechanical behaviour for two reasons; first, the connection to the city wall and adjacent buildings is asymmetric; second, the building clearly exhibits signs of the two independent construction phases. Even today, the ancient defence tower can be recognized to the east of the gate (Fig. 2): the plan is C-shaped, 7.8 m by 4.5 m, and the height is 25.6 m. Endoscopic tests showed that the two parts of the masonry body exhibit completely different stratigraphic and mechanical
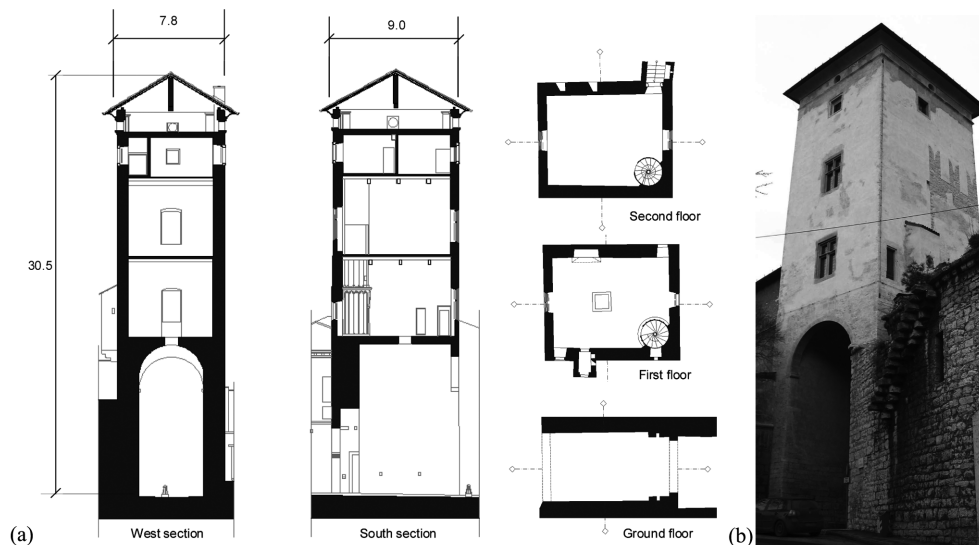


Fig. 1 (a) Plan view and cross sections of Torre Aquila and (b) overview of the tower
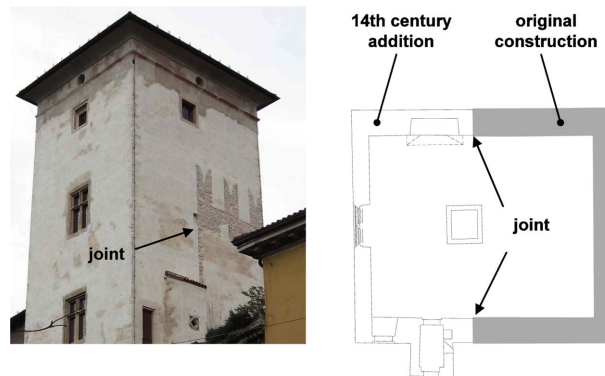
Fig. 2 Structural joint in the wall of the tower

properties (Zonta *et al.* 2008). In detail, the lower level walls are 40 cm thick, made of stone blocks and with an incoherent wall filling. At the upper levels, the older portion of masonry is thick stone blocks, while the more recent part is brick and stone blocks of different sizes. However, based on the past investigation, we are still cannot confirm whether the two bodies of masonry are structurally connected or not through the joint.

Today the castle is open as a historical museum, and the Aquila Tower attracts thousands of visitors every year due to a cycle of frescos, called "the Cycle of the Months", on the second floor (Fig. 3). This consists of a total of 11 decorated panels describing courtly scenes and typical



Fig. 3 Fresco of Cycle of the Months: June. Torre Aquila, Castello del Buonconsiglio, Trento, 3.05×2.04 m
(Courtesy of the *Castello del Buonconsiglio Monumenti e collezioni provinciali.* Copyright reserved)

working conditions in different months of the year in ancient times (one month is missing due to the existence of a winding stair connecting the first floor and the third). These frescos are recognized as a unique example of non-religious medieval painting in Europe.

The main source of concern for the local conservation board is the preservation of this artwork, in view of possible future tunneling under the Buonconsiglio Castle area. The Castle is located at the edge of the historic center of Trento and in the past the Aquila Gate was the main entrance to the city from the east. With the expansion of the city in the second half of the 19th century, most of the eastern city wall was demolished and the entrance to the city was moved a few hundred meters south of the original gate. Today this solution is inadequate for the amount of traffic. The solution to this problem, pursued by the Municipality of Trento, is to bypass the Buonconsiglio Castle with a road tunnel. The tunnel has been long delayed not only for its high cost, but also due to the concerns of the Conservancy over the safety of the Cycle of the Months. Tunneling could cause unwanted subsidence of the Castle foundations, and also vibration which is critical to fresco preservation.

It is not clear when or even if tunneling will start: as a precaution, the castle owner accepted the idea of installing a permanent monitoring system, to warn of potential risk to the frescos, whatever the source. In terms of sensors, this system would include accelerometers and deformation gauges, with a number of environmental sensors to compensate for temperature effects; system operation also needs appropriate algorithms to process the acquired data and make them available to the user in real-time.

When starting system design, there was discussion whether to use a WSN rather than a traditional cabled based system. The many pros of WSN, and specifically the very low impact of the installation, all favoured this solution. On the other hand, at the time WSN technology was justly judged not mature enough for long-term monitoring: this route implies use of an experimental system needing much development and possibly downtime for debugging and adjustment of software and hardware. Accepting the possibility of downtime during the first year of system operation, the owner eventually agreed to the WSN-based solution. The technical details of the system later deployed in the tower are described in the next Section.

## 3. Design and installation of the wireless monitoring system

### 3.1 Sensor network requirements

We can summarize as follows the challenges met in designing the sensor network for permanent monitoring of this historic tower:

(1) There are five floors, and many spatially distributed sensors are needed on the different levels to fully understand the conditions of the tower. With a single sink on the top floor, it is difficult and expensive to link each node directly to the sink. Therefore, a multi-hop WSN is needed for reliable and energy efficient wireless communication. In addition, there are various possible ways for a source node to reach the destination for data transmission, so an effective topology algorithm is needed to realize a flexible and optimum wireless communication route network.

(2) The whole system is a multi-scale WSN including different types of spatially distributed sensors (deformation sensor, environmental nodes and accelerometers), whose setups and operations are quite different. The deformation sensors are deployed to monitor the static

deformation of the tower, and can work at a low sampling rate. The same holds true for the environmental nodes. However, in order to gain dynamic properties of the tower, accelerometer nodes have to work at a much higher sampling frequency. This will result in a large amount of data, which needs an efficient local processing scheme to reduce data transmission, as well as an intelligent network algorithm to achieve maximum usage of the limited bandwidth source in the network.

(3) In a long term monitoring system, the life span of each node will be critical. Frequent change of batteries is not admissible, not only due to difficulty or danger of reaching the installation positions, but also to limit invasiveness and reduce maintenance costs. Effective use of limited power in a network needs dedicated hardware design, and an intelligent and efficient network algorithm using power only as necessary is also of prime importance.

(4) For acceleration data, sampling synchronization is a critical issue for the vibration nodes, to allow correlation analysis between information from different nodes. This is difficult, due to the time drift between nodes, and after analysis, we selected 10% of a sampling interval (0.5 ms) as the largest time drift.

(5) In a historical tower, access to adjust the sensor network each time is not admissible. In special cases, such as in the presence of many tourists, a particular network configuration adjustment could be necessary. Therefore, a remote tasking capability is indicated to enable remote control of system configuration.

As remarked in the introduction, most off-the-shelf wireless platforms or hardware do not offer the performance fulfilling the above requirements. To make up for this gap, a low cost and long lifespan wireless sensor network with customized hardware design, integrated with highly reusable and easily extensible software services has been developed, specifically for long term structural health monitoring.

### 3.2 Hardware

In the wireless unit, we selected 3MATE! WSN module (Fig. 4(a)), developed by TRETEC (www.3tec.it), as the core platform to provide the computational core and wireless communication functions. The 3MATE! is a TMote-like (Polastre *et al.* 2005) device, which is an ultra low power wireless sensor module. At the core of this mote, the Texas Instrument 16-bit MSP430F1611 microcontroller, at the peak of their product classes, is chosen for its on-chip hardware peripheral. The module has an 802.15.4-compliant radio chip and an internal microstrip antenna. The integrated radio is capable of data rates of 250 kBps and can communicate up to 50 m indoors and 125 m outdoors, with the onboard inverted-F microstrip antenna. The power supply voltage can range from 2.1 V to 3.6 V with a power consumption of a few milliwatts in active mode and microwatts in standby mode, permitting the use of two 1.5 V batteries in the normal AA, C or D sizes for up to one year of lifetime. The vibration sensor modules also had an additional 32 kByte FRAM chip to allow for energy-efficient temporary storage of vibration readings. Unlike traditional flash technology, FRAM provides faster read/write operations and a much higher number of read/write cycles with lower power consumption. The only disadvantage is its relatively lower storage densities than Flash devices and its limited storage capacity. In our design, a central sink was adopted to collect and store all the measurements from different nodes. Once the sampling process and data transmission in a session finish, the FRAM could be released for use in the next session.

The 3MATE! node with an additional FRAM chip is power efficient, with a demand below 3 $\mu$A
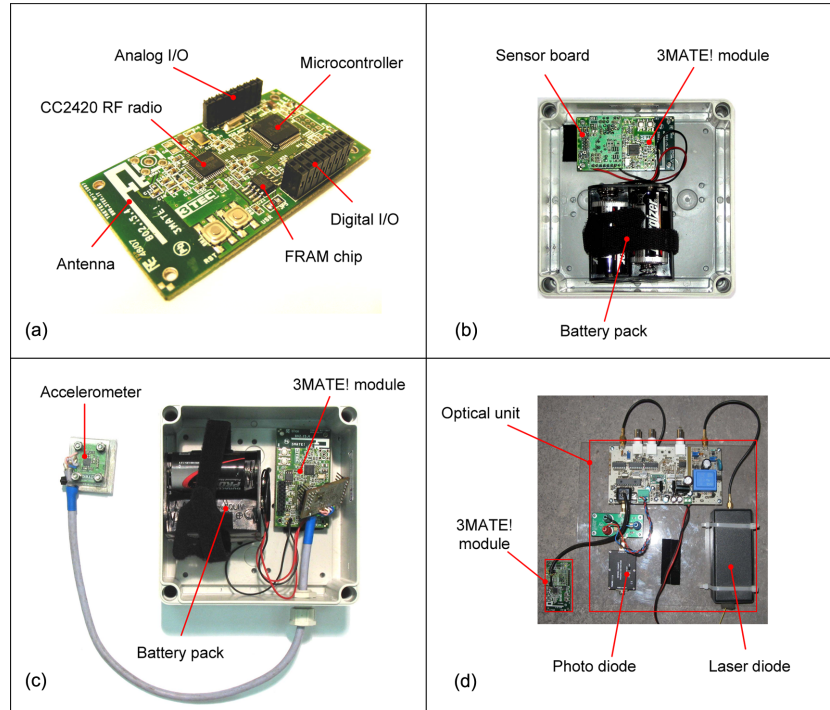
Fig. 4 Hardware components of the system: (a) 3MATE! module, (b) environmental node, (c) accelerometer node and (d) fiber-optic deformation node

in sleep mode. During sampling mode, the current needed is below 3 mA, and up to 20 mA during transmission. Power consumption can be further limited by selecting only enough transmitting. The communication protocol implemented in the firmware allows a very low duty cycle of the communication task with very low impact on the overall power efficiency. Except for the two special deformation nodes described in Section 3.5, all nodes were designed to work for around one year with two pairs of D or C batteries. In the specific case of Torre Aquila, changing batteries every year is perfectly acceptable, as this operation has very low impact on the routine maintenance normally carried out in the Castle. Each node costs about 80 euro.

### 3.3 Environmental nodes

In its simplest configuration, the basic 3MATE! module has an extension board for environmental monitoring, with simple analog temperature, relative humidity and light sensors (Fig. 4(b)). In the specific application the only parameter required was temperature. The sensor measurement range is -40 °C to 125 °C with an accuracy of 0.5 °C.

### 3.4 Acceleration nodes

The accelerometer is based on a Freescale compact tri-axial sensor, using Micro Electro Mechanical Systems (MEMS) technology. Even if most recent MEMS accelerometers are widely available in digital read technology, an analog version was selected with an output voltage of

800 mV/g in 1.5 g range mode. Power consumption is approximately 1 mW, at supply voltage 2.2~3.5 V, and reduces to few microwatts in standby-mode. Unlike digital, the analog output allows the signal to be coupled with an analog front-end for further signal amplification and filtering with a resulting resolution of 0.1 mg. A/D conversion is performed by the A/D converter already integrated in the standard the 3MATE! module. Most commercial mote-based acceleration nodes fit the sensor on the wireless board or on an extension directly attached to the wireless unit. This solution is sometime preferred because it allows very simple and compact packaging. However, in this case the accelerometer response is affected by the mechanical impedance of the board/packaging system, a condition not normally acceptable in vibration monitoring of civil structures. To overcome this problem, in our design the accelerometer is mounted on an independent rigid support, anchored using glue or expansion bolts to the surface to be monitored. The accelerometer is connected to the main board with a short cable, allowing for maximum flexibility during sensor placement (Fig. 4(c)). Before installation, all the vibration nodes were calibrated on a small shaking table excited by harmonic pattern at different frequencies. During the test, the wireless accelerometer is mounted back to back with a pre-calibrated single axis standard reference accelerometer (Fig. 5(a)), which in the specific case is a piezoelectric PCB transducer, model 393B12. For each node and axis, comparison between the reference and actual signals allows calculation of the linear compensation coefficient that renders the two amplitudes identical (Fig. 5(b)); the calibration constant calculated is then recorded and later used for online compensation.

## 3.5 Deformation nodes

Here, as in any permanent monitoring system, the long term stability and reliability should be addressed with special attention not only for wireless communication but also for sensor devices. Due to their long-term stability, durability and immunity to most environmental attacks, Fiber Optic Sensors (FOS) have in the last decade attracted much attention in health monitoring of civil structures. For the reader who is not familiar with the topic, good overviews are in the textbooks by Measures (2001) and by Glišić and Inaudi (2007); but see also as sample applications Lee (2003), Sohn *et al*. (2003), Inaudi (2005), Bastianini *et al.* (2006), Inaudi and Glišić (2008). However, the generally high cost of the interrogation unit, of the order of tens of thousand of euros, is possibly
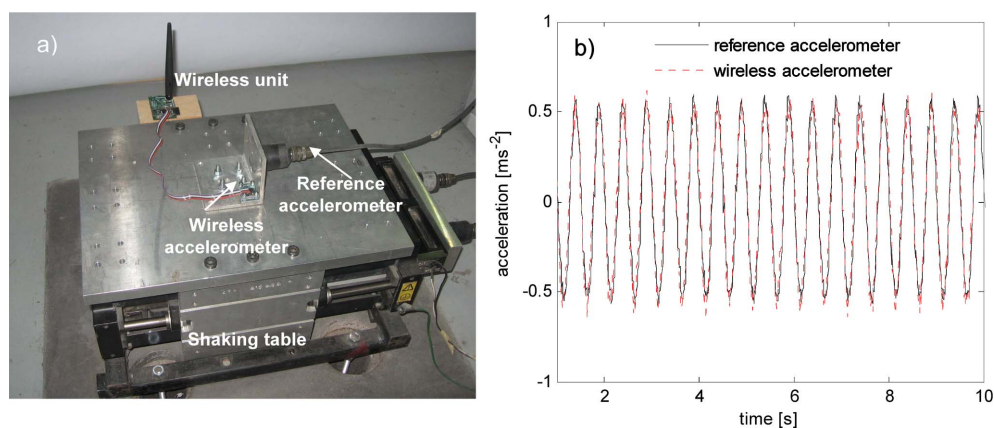


Fig. 5 (a) Calibration test setup and (b) sample result for vibration nodes

the largest obstacle to wide application of FOS in real cases (Casas and Cruz 2003). In a large scale deployment, this cost can be justified by the high number of channels that can be interrogated at the same time by a single unit, taking advantage of the multiplexing capabilities of optical technology.

However, in practice, multiplexing implies physically wiring the remote optical sensors to a central unit, where the optical signal is demodulated and converted to digital. We can easily understand that such a multiplexed scheme is *per se* against the WSN paradigm, where the analog to digital conversion occurs locally in order to transmit the signal wirelessly. Thus, when we attempt to integrate an optical sensor into a wireless network, in principle the only logical scheme is to integrate one interrogation unit for each optical wireless node. From the economic point of view, this scheme is not sustainable, given the high cost of commercial interrogation units.

To overcome this problem, we developed for this application a low cost FOS technology for use with a single-channel interrogation unit. The sensing principle is to measure the optical path unbalance between a measurement fiber, fixed to the structure and a reference fiber, kept loose, by detecting the time-of-flight delay of a laser pulse split into the two optical circuits.

The optical components of the sensors are inexpensive bare fibers, and to further reduce costs, we employ off-the-shelf components in the interrogation unit: a nanosecond laser pulser, a photo-diode and a Pulse Width Modulation electronic circuit. Fig. 6 illustrates schematically the working principle of the system. A function generator drives the laser diode to emit a sequence of optical pulses (more specifically, the interrogation unit used for this application generates 1 ns pulses at 30 kHz). The resulting optical signal is split at the first coupler into the measurement and reference fibers, and then recombined at the second coupler. Because of the difference in length of the two optical paths, once recombined the pulse sequence is duplicated with a time delay proportional to the path imbalance. In the interrogation unit, the optical pulse sequence is transduced back to electric at the photo diode, and used to drive a flip-flop, which in turn controls the output voltage of the interrogation unit. Any elongation of the measurement fiber results in a change in the time-of-flight delay of the optical pulse and therefore in a change in the output voltage at the interrogation unit, which is theoretically expected to be linearly proportional. The reader is referred to Pozzi *et al.* (2008) for a more detailed description of the opto-thermo-mechanical relationships which link elongation to optical path imbalance.

The system was developed in a number of prototypes and tested in the laboratory to validate its
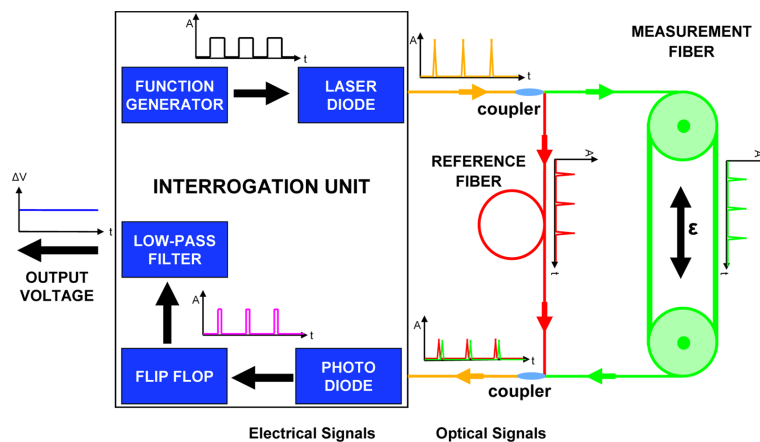


Fig. 6 Layout of the of the time-of-flight fiber-optic sensor system
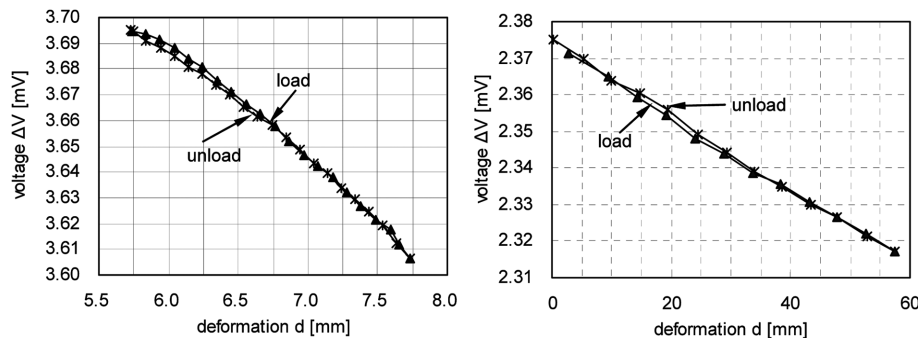
Fig. 7 Outcomes of the calibration of the two fiber-optic deformation sensors: (a) coil sensor and (b) long FOS

performance. More specifically, two optical arrangements were produced for this application: the first is a 100 m long optical fiber coil, designed for a measurement base of about half a meter, the second is a 15 meter gauge-length sensor. Both FOS were interfaced with the standard 3MATE! unit to provide wireless communication (Fig. 4(d)). In order to quantify the linear coefficients between deformation and electrical signal, both FOS were calibrated in the laboratory before installation (Wu 2009), and the calibration results are fitted for the coil sensor and for the 15 m long FOS respectively (Fig. 7). The test results show that system response is almost linear with precision of the order of 20-60 $\mu\varepsilon$. The nonlinear response observed for the coil sensor at low elongation levels is due to uneven pretensioning level of the fiber wraps, some of which are in a loose state. For higher elongations, when all the loops are appropriately pretensioned, the system exhibits good linear response.

### 3.6 Layout of the system

The WSN installed in the tower consists of 16 nodes, distributed on all the floors as shown in Fig. 8(a), plus one base station on the third floor, which is the gateway between the local network and Internet. The number and type of sensors in consistent with the specific requirements stated in Section 3.1. To record the vibration induced in the building, three acceleration nodes, #144, #145 and #146, were deployed, compliant with DIN 4150-3 standard (DIN 1999): specifically, one is located on the ground floor, while the other two are installed on the top floor to record the acceleration response of the tower (Fig. 8(b)).

Due to the asymmetric structural response of the building and the existence of the joint, an optical elongation sensor (node #154) was deployed along the southern wall to monitor possible joint opening on the 1st floor (Fig. 8(d)): the model adopted is the 100 m-long optical coil described in Section 3.5, pretensioned on two support wheels, anchored to the wall using expansion bolts. In order to detect elongation of the tower resulting from possible non-uniform subsidence, another 15 m-long FOS was installed along the south-west wall corner, from level +11.7 m to level +26.8 m. Details of the top and bottom anchorages of the sensor are shown in Figs. 8(e) and (f) respectively. An extension of the optical fiber enters the tower through the roof and connects to the deformation node #153, located on the top floor.

Apart from the above sensors, 11 additional nodes (Fig. 8(c)) are distributed on the floors to monitor temperature; the number of environmental nodes is redundant, because some of them serve as bridge nodes in the communication network.
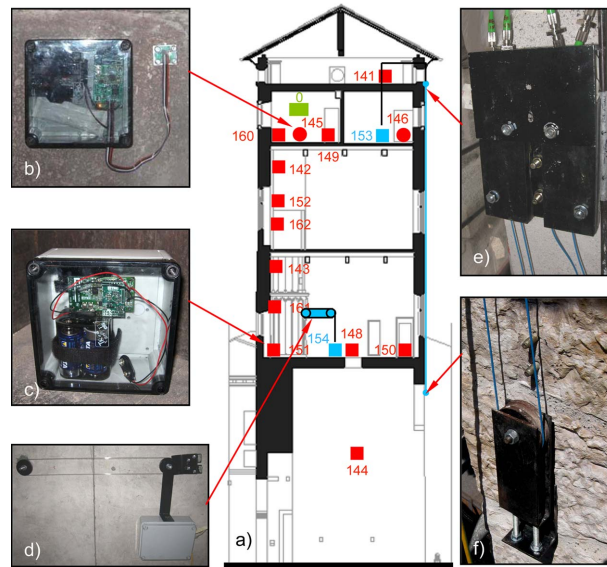
Fig. 8 WSN deployment in Torre Aquila: (a) south cross-section of the tower indicating the nodes position, (b) accelerometer node, (c) environmental node, (d) optical coil sensor installed, (e) details of top and (f) bottom anchorages of the long FOS

Table 1 Node types and their corresponding configurations

| Node tupe | Number | Operating parameters | Assigned value | ID |
|---|---|---|---|---|
| FPS node | 2 | Sampling period | 1 min | #153, #154 |
| Acceleration node | 3 | Sampling frequency | 200 Hz | #144, #145 #146 |
| | | Sampling period | 10 s | |
| | | Number of sampling session per day | 36 | |
| Environmental node | 11 | Sampling period | 1 min | #141, #142, #143, #148, #149, #150, #151, #152, #160, #161, #162 |
| Sink node | 1 | | | #0 |

As explained in Section 3.7, the system allows remote tasking of the data acquisition parameters. Table 1 summarizes the parameters currently applied: in detail FOS and environmental nodes are interrogated every minute, while acceleration is recorded in a series of sessions with a sampling frequency of 200 Hz lasting 10 sec each; currently the system performs a session every 45 minutes.

## 3.7 Software

At the software level, we built all application services on top of our TeenyLIME middleware (Costa *et al.* 2007), which provides an abstraction layer on top of the operating system running on each single node. The application modules interface with a shared memory space spanning neighbouring nodes in communication with each other. The interaction among components takes place by means of insertion, removal and reading of tuples, units of information arranged as ordered
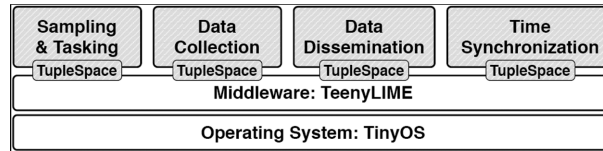
Fig. 9 Software architecture

sequences of typed fields; moreover, a reactive primitive enables listening for changes in the distributed tuple space. This software layer allows the design of decoupled and reusable application components resulting in a reduced implementation burden for the developer and a smaller memory footprint with respect to services built directly on top of the operating system. Based on this software architecture (Fig. 9), we implemented the modules required to satisfy the application needs.

To handle the sensor heterogeneity, we devised a data collection protocol that efficiently handles different traffic patterns (Ceriotti *et al.* 2009). The high volumes of data produced in bursts by the accelerometers demand highly delivery, as sample losses can damage signal reconstruction; whereas the lower sampling rate of temperature and deformation nodes sets lower demands as occasional losses are acceptable. The general system functions are also checked, and for example, the battery levels at each node were recorded. To achieve this, the routing protocol builds a tree topology, rooted at the sink, which is refreshed periodically to account for connectivity changes; the metric used to construct the paths is based on a link quality index that allows nodes to choose the routes with the highest probability of successful data forwarding (an example of routing topology is shown in Fig. 10). In addition, we apply a hop-by-hop recovery scheme to account for losses in the communication channel. In this scheme, each message sent from a child to its parent in the routing tree, is tagged with a sequence number; moreover, each node keeps a cache of the last messages forwarded. When the parent recognizes a gap in the sequence numbers of the messages received, it accesses the corresponding child cache, recovering the missing information.
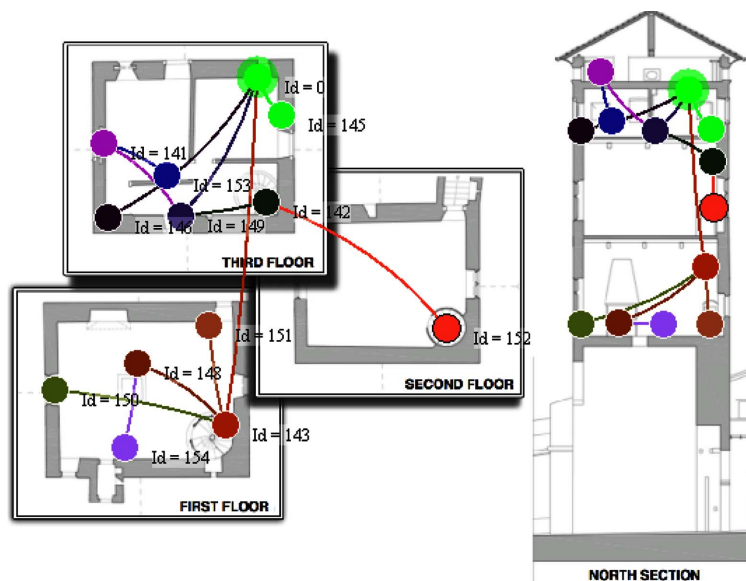


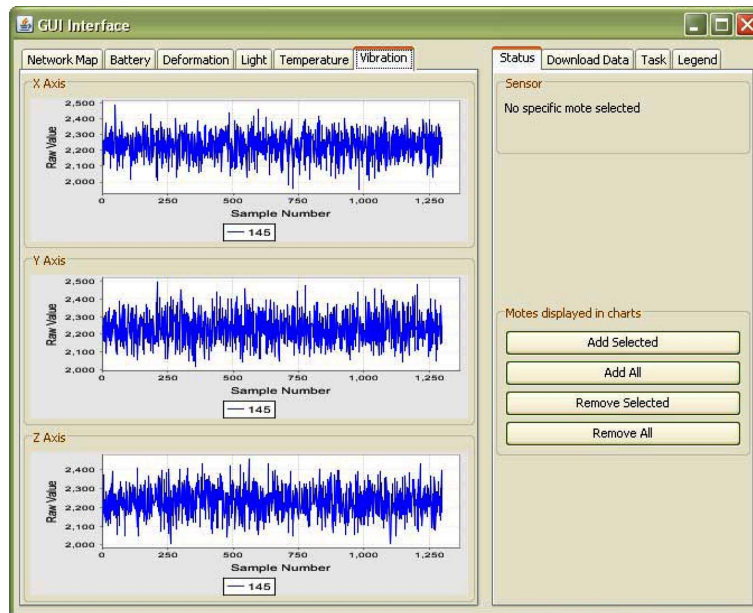Fig. 10 Example of the optimized tree topology

Fig. 11 Graphical user interface (GUI)

When sampling vibration signals at multiple nodes, time synchronization is a common issue in WSN, which has to be properly addressed for an effective correlation analysis at different sensors. Among several available protocols, here we adopted a modified version of the solution described in the paper by Ganeriwal *et al.* (2003). The nodes are organized in hierarchies where the root provides the reference time. Each member periodically synchronizes with the next higher level in the hierarchy, preventing clocks from drifting too far from each other. With this simple solution it is easy and efficient to control the synchronization error within the time drift tolerance as required by the application. While this system component is typically placed near the operating system to provide the required accuracy, we efficiently and effectively implemented it on top of the TeenyLIME middleware.

Finally, the system provides a remote tasking functionality that disseminates throughout the network the operating parameters controlled by the user to tune the configuration of the network. This is particularly necessary not only in the cases where an adjustment is required due to unusual environmental effects, but also in daily maintenance of the whole network. All the tasks can be remotely established by the person responsible for the data analysis by means of a custom graphical user interface (Fig. 11), from which the data acquired from the network can be also visualized online.

## 4. Data collection and analysis

### 4.1 Overview of data recorded

The wireless sensing system was first installed in September 2008 and underwent an initial period of examination, debugging, adjustment and updating of the monitoring system.

After installation of the final version of the software, on April 15, 2009, the system worked continually save for battery replacement in August 2009. Data corresponding to environmental phenomena,
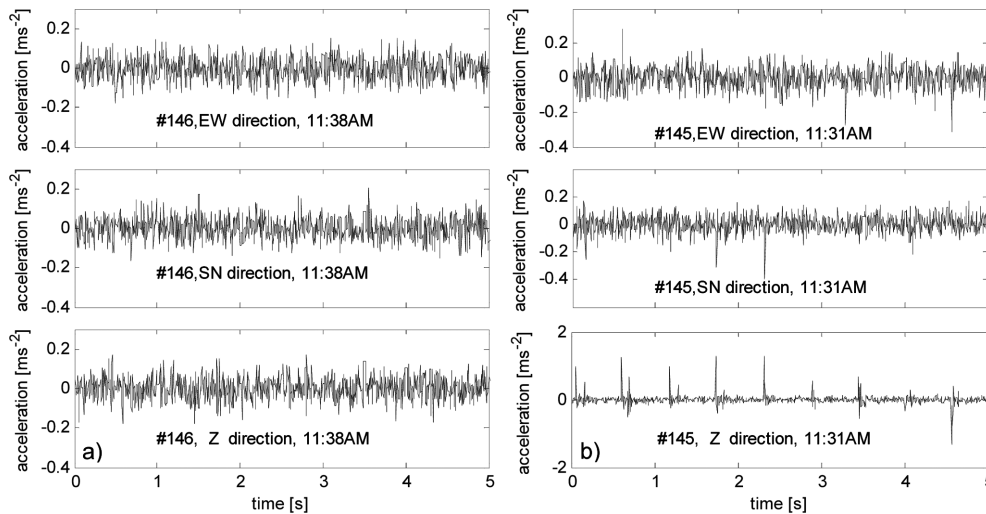
Fig. 12 Sample acceleration signals recorded at node #146 under pure ambient vibration (a) and at node #145 when people walking nearby

tower deformation and dynamic vibration behaviour were monitored and acquired continuously except during the maintenance periods. In order to check transmission reliability, data loss is monitored continuously. In recent months, the overall loss rate is assessed at less than 0.01%. This is good performance if compared with other long-term wireless sensor network deployments reported in current literature (Ceriotti *et al.* 2009).

In order to monitor the day by day level of vibration at ground level and on the top floor of the tower, every day a number of sampling sessions were acquired, each 30 seconds long. As an example, Fig. 12(a) shows part of one typical signal acquired in normal environmental conditions in three axes recorded at node #146 (located at the top floor) at time 11.38 AM. We see immediately that the amplitude of ambient acceleration is very low, less than 0.2 ms$^{-2}$. For a qualitative idea of the acceleration level recorded, compare Fig. 12(a) with the graph of Fig. 12(b), acquired under similar conditions with one person jumping near the sensor (in z direction). The graph of Fig. 13 shows the FFT of two of these signals expressed in *spectral velocity* and on a logarithmic scale (*spectral velocity* is the quantity commonly used by industrial standards to state vibration limits). On the same graph we also show the vibration limits, suggested by BS 7385-2 and DIN 4150-3 standards (BSI 1993, DIN 1999), for structures sensitive to vibration, such as an historic building. By examination of this graph, we observe that the typical ambient vibration recorded is well below the limits recommended, and lets us conclude that vibration is currently not a source of concern for the stability of the tower, nor even for integrity of the frescos.

To evaluate the response of the FOS, it is useful to compare the measured response with that estimated a priori before installing the monitoring system. A three-dimensional Finite Element Model (FEM) of the tower was developed in (Zonta *et al.* 2008) and used to simulate its response under different load and environmental conditions. The outcomes highlight that, compared with other effects such as wind and snow, thermal gradients produce the largest absolute strain in the tower, although only a minor part of this is stress-induced. For example, the thermal distortion of the crack is estimated as 0.157 mm on a summer day, and 0.069 mm in winter; while the response of the same sensor induced by a 10 mm settlement at the southwest foundation is estimated to be
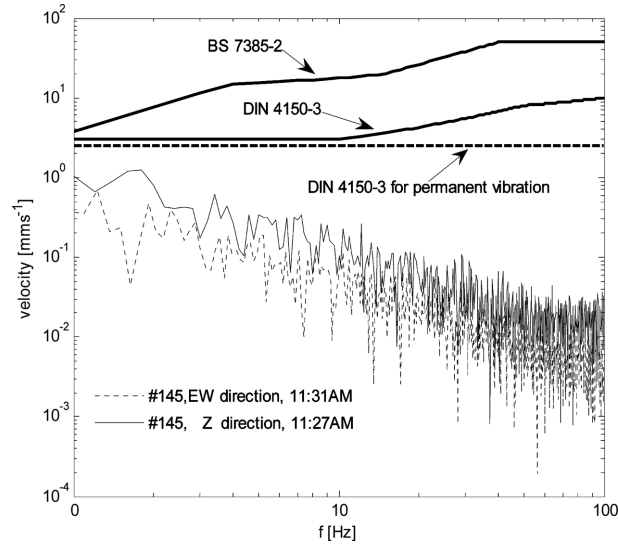
Fig. 13 Fourier spectrum of typical acceleration records, compared with vibration limits recommended by BS 7385-2 and DIN 4150-3 standards (BSI 1993, DIN 1999)

only 0.0023 mm. This and similar observations suggest the importance of temperature compensation for correct evaluation of structural response as provided by the monitoring system. Fig. 14 shows the deformation records from two FOS with their corresponding temperatures. Fig. 14(a) presents the deformation measured by the coil sensor (node #154) from September 2008 to September 2009. The daily variation is between 0.05 mm on a cloudy day and 0.30 mm when sunny, and this is in good agreement with the numerical results of the FEM model. Similarly, Fig. 14(b) shows the FOS elongation and temperature recorded at node #153 in the same period (observe that the long FOS
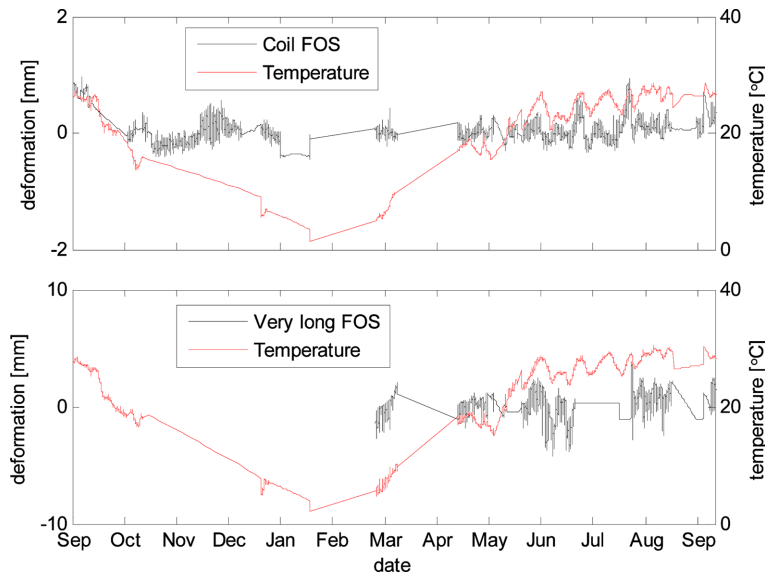


Fig. 14 Time histories of deformation recorded by coil FOS (top) and long FOS (bottom)

was operating only after February 2009). Compared with the predicted value in the deformation presented in Zonta *et al.* (2008), the acquired measurements are of the same order of magnitude.

### 4.2 Temperature compensation

As mentioned, the main objective of monitoring is the preservation of the artistic frescos located at the second floor of the building. Damage to frescos is caused essentially by stress-induced strain: we must therefore compensate the strain measurements to eliminate the temperature effect. To do this, it is convenient to separate the temperature record into two components: the daily variation and the seasonal trend. Daily variation affects the tower in a non-uniform way, producing significant distortion of the tower; while the seasonal trend is a slow steady change in temperature, resulting in uniform expansion or contraction of the structure. The effect of daily and seasonal variation has been quantitatively explained in Zonta *et al.* (2008) with the support of the FEM.

A rough but effective way to extract the seasonal component is to select one sample per day at the time before sunrise; while evidently the daily excursion is given by the difference between the record and the seasonal trend. Fig. 15 illustrates this process as applied to sensor node #154, the coil sensor placed across the joint, in the period June 1 to July 31, 2009. By comparison of the elongation record shown in Fig. 15(a), with the daily and seasonal components of the temperature variation shown in Figs. 15(c) and (d), we can qualitatively appreciate how the structural deformation is mainly correlated to the daily variation.

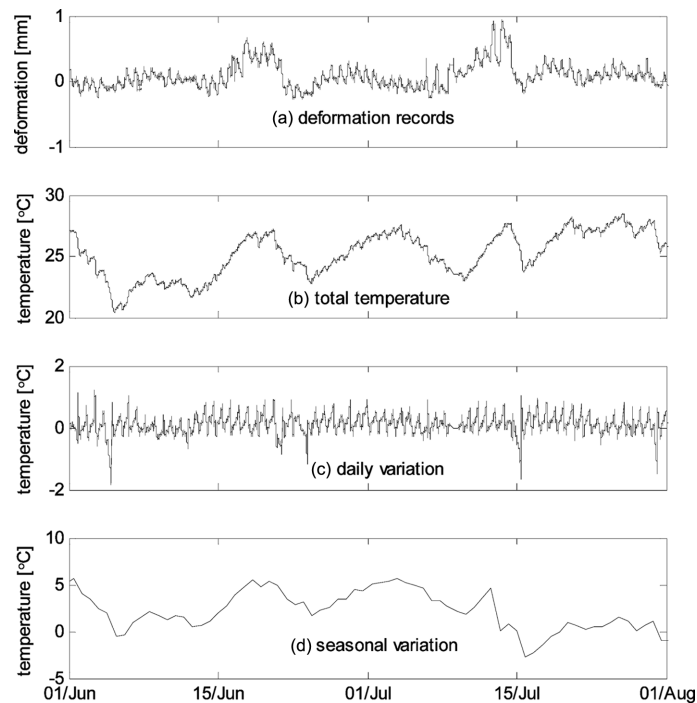In order to remove the temperature dependent variation from the raw elongation measurements,



Fig. 15 Deformation history recorded by optical-coil sensor, (a) node #154, (b) temperature history recorded at the same node, (c) daily and (d) seasonal components

we applied an algorithm based on Bayesian logic. Suggested readings for those interested in this topic, and its application to structural monitoring, are Sivia (2006), Beck and Katafygiotis (1998), Beck and Au (2002), Papadimitriou *et al.* (1997), Sohn and Law (1997). Here, we will follow the same general approach already proposed in Zonta *et al.* (2008): the thermometers are viewed as *environmental sensors*, recording the environmental action, while the two FOS are regarded as *response sensors*, recording the structural response of the tower to this action. In order to remove temperature dependent effects, we organize the time history into a series of time intervals of one day, with the assumption that this time span is small enough to consider the compensated response as constant within this interval. The recorded deformation history is assumed to have a linear relationship with both daily and seasonal temperature variation, although, because of the different mechanism explained above, the two linear coefficients are considered independent. Thus, the relation between a deformation sample $m_T(t)$ recorded at day $T$ and time $t$, and the compensated response $m_T^o$, supposed to be constant within day $T$, can be formally written as

$$m_T(t) = m_T^0 + \alpha_T^d h_T(t - \Delta t_d) + \beta^s h_T(t - \Delta t_s) + n_T(t; \sigma_T) \qquad (1)$$

where: $\alpha_T$ is the linear coefficient relating deformation and daily temperature variation $^d h_T$, $\beta$ is a linear coefficient between deformation and seasonal temperature variation $^s h_T$; $\Delta t_d$ and $\Delta t_s$ are the time lags between the deformation and the two temperature components; and $n_T$ is a Gaussian noise with zero mean value and standard deviation $\sigma_T$, reproducing instrumental and environmental disturbances.

We can rewrite Eq. (1) for any of the samples acquired at day $T$, obtaining a set of equations with unknown parameters $[m_T^0, \alpha_T, \beta, \Delta t_d, \Delta t_s, \sigma_T]$ which can be reasonably assumed constant within time interval $T$. The above parameters, including the compensated deformation, all regarded as uncertain variables, can then be estimated by a classical Bayesian identification procedure. This procedure can be repeated day by day, eventually obtaining a record of compensated measurements.
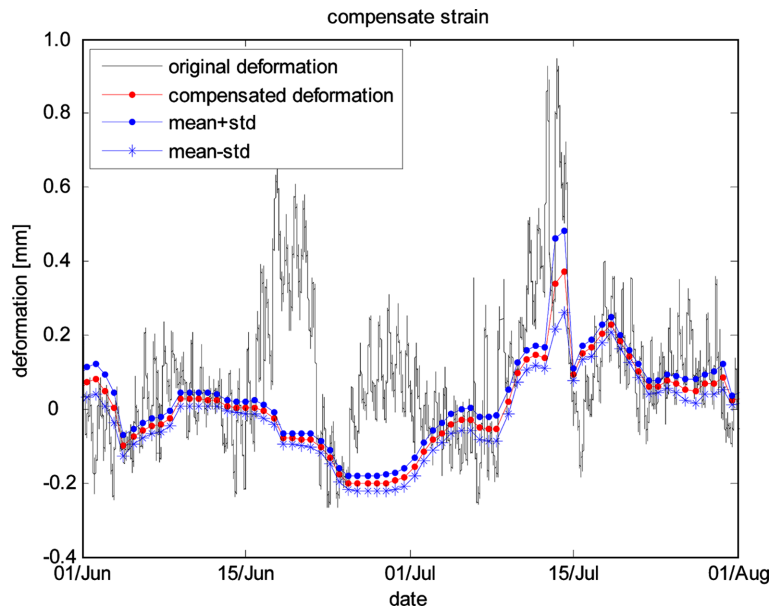


Fig. 16 Estimate of compensated deformation from optical coil sensor (node #154)

As an example of this process, Fig. 16 illustrates how this procedure applies to the response of the coil FOS (node #154), in the period from June 1 to July 31. In detail, the red plot is the day-by-day best estimate of compensated deformation $m_T^0$ based on all the past information, while the blue lines indicate the best estimate plus or minus its standard deviation respectively, and give an idea of the degree of confidence of this information. More specifically, the system estimates $\alpha_T$ to be 0.1 mm C$^{-1}$ with standard deviation of 0.04 mm C$^{-1}$, and $\beta$ to be 0.05 mm C$^{-1}$ with standard deviation of 0.02 mm C$^{-1}$. It worth noting that during the updating process, coefficient $\alpha_T$ is typically bigger than $\beta$, which confirms that, as observed before, for identical temperature excursions, the daily component always produces greater changes in deformation than the seasonal. The observed variation of the compensated strain is relatively small, of the order of 0.2 mm, confirming, as expected, that so far the tower is not undergoing any significant deformation.

### 4.3 Data evaluation

To prevent possible damage to the frescos, specifically in view of the future tunneling that motivated the deployment of this system, it is important to recognize early any anomalous condition states of the tower. For example, linear trends in deformation are a typical sign of ongoing phenomena that should be under control. To recognize in real time a linear trend of deformation, we can further apply a Bayesian algorithm to the compensated records (Zonta *et al.* 2009). As the monitoring system continues to work, more and more data become available. A Bayesian algorithm lets us update the past estimate of the tower condition with the fresh data acquired. Here again we take deformation node # 154 as an example to demonstrate the method. In principle, we expect the tower to behave according to one of the following two alternative scenarios: (1) the joint does not open, thus the deformation recorded at sensor #154 stays constant; (2) the joint is opening and the measurement exhibits a continuous increase. More formally, we can model the behavior of the joint in the two scenarios as follows

$$
\begin{cases}
m_T^0 = d_1 & \text{in } S_1 \\
m_T^0 = k \cdot T + d_2 & \text{in } S_2
\end{cases}
\tag{2}
$$

where $d_1$ is the constant deformation expected in scenario $S_1$, and $d_2$ and $k$ are the offset and linear trend of deformation in scenario $S_2$. We recognize that each scenario depends on a set of parameters, which can be formally expressed as $X_1 = [d_1]$ and $X_2 = [k, d_2]$. Now, our problem is to estimate the probability of being in one scenario, $S_1$ or $S_2$, based on the fresh data acquired daily. Say that we are at day $T$, and we acquire the new data $m_T^0$. Based on whole set of data $\{m_{T-1}^0\}$ acquired up to the previous day $T$-1, we already have an estimate of the probability $\text{prob}(S_n|\{m_{T-1}^0\})$ of being in one of the two scenarios. This probability is regarded as *prior probability*, and represents our knowledge *before* analyzing the current data. Once acquired the last sample, Bayes' theorem allows us to estimate the new (or *posterior*) probability based on the *prior* one, according to

$$
\text{prob}\left(S_n \middle| \{m_T^0\}\right) = \frac{\text{PDF}\left(m_T^0 \middle| \{m_{T-1}^0\}, S_n\right) \cdot \text{prob}\left(S_n \middle| \{m_{T-1}^0\}\right)}{\text{PDF}\left(m_T^0 \middle| \{m_{T-1}^0\}\right)}
\tag{3}
$$

where PDF is the short form for Probability Density Function. In order to make this algorithm work in practice, we need to calculate the different terms in Eq. (3). The first term in the numerator, referred to

as *scenario evidence* (sometimes also named *scenario likelihood*) of scenario $S_n$, representing the probability of occurrence of the data if the specific scenario is given, can be calculated by integrating over the whole parameter domain $DX_n$, using the marginalization and product rule

$$\text{PDF}\left(m_T^0 \Big| \{m_{T-1}^0\}, S_n\right) = \int_{DX_n} \text{PDF}\left(m_T^0 \Big| X_n, S_n\right) \cdot \text{PDF}\left(X_n \Big| \{m_{T-1}^0\}, S_n\right) \cdot dX_n \qquad (4)$$

The denominator term, usually referred to as *evidence*, is a normalization term, that warrants that the sum of the probabilities of being in the different scenarios be 1. The prior probability at the first interval should reflect our prior judgment about the problem; in the absence of any other information a uniform distribution should be assigned. For details of the algorithm, the reader is referred to (Zonta *et al.* 2009).

Fig. 17 shows, again in the period from June 1 to July 31, how this approach applies to the compensated signal from deformation sensor #154. The first graph, Fig. 17(a), plots the posterior probability of scenario $S_2$ estimated day-by-day based on the past data: in simple terms, this graph quantifies the possibility of having a linear trend of deformation. As expected, to date this value
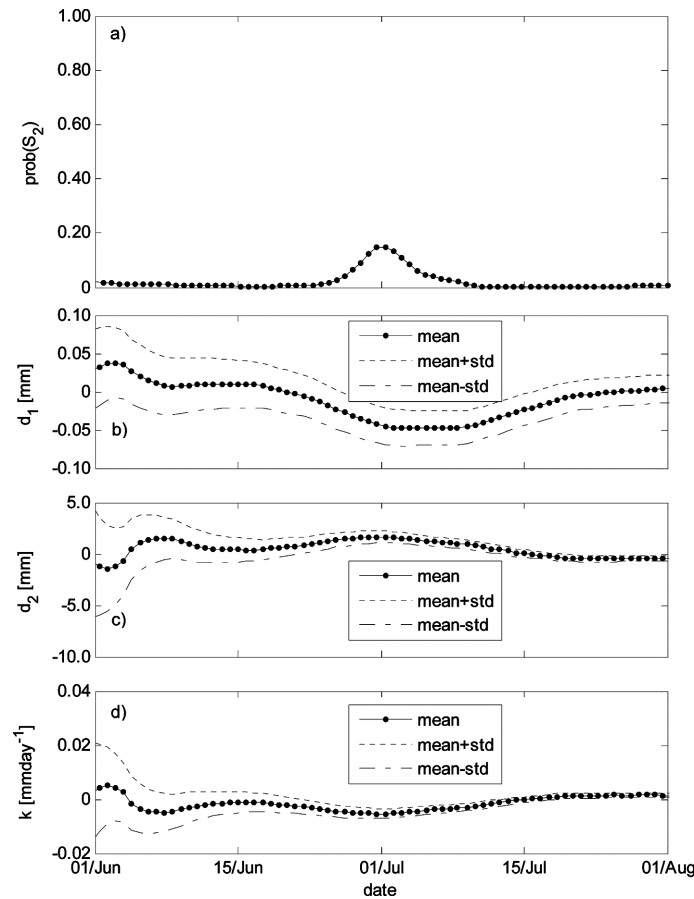


Fig. 17 (a) Posterior probability of Scenario 2, (b) best estimate and distribution of parameter $d_1$ (baseline deformation) in Scenario 1, (c) best estimate and distribution of offset $d_2$ and (d) linear trend $k$ in Scenario 2

remains for most of the time close to zero; once only, when the deformation record exhibits sharp changes, this probability departs from zero reflecting some temporary concern, and immediately returns when new data are available. Using the same Bayesian approach, we can also calculate the posterior distribution of the scenario parameters. As shown in Fig. 17(b), assuming Scenario 1, 'no trend', to be correct, the estimated values of permanent deformation rapidly converge to 20 $\mu$m, with a standard deviation of 6 $\mu$m. It is likewise interesting to observe that, assuming correct Scenario 2, 'linear trend', the most likely estimate of the linear trend $k$ converges after 20 days to a value of 0.002 mm day$^{-1}$, corresponding to an annual trend of 0.29 mm year$^{-1}$. Of course, this value, and the corresponding likelihood, are both too small to call for an urgent action on the tower.

## 5. Conclusions

We presented an application of WSN technology to monitor permanently Torre Aquila. This effort was motivated by the need to keep under control the structural response of the tower, in terms of deformation and vibration, to preserve the integrity of the valuable artworks located inside, in view of possible future tunneling work.

The specific application, and the long-term requirement, demanded the development of customized hardware and dedicated software. As for hardware, the 3MATE! wireless sensor module was selected as the core platform, to allow reliable wireless communication at low cost and with a long service life. In terms of software, a multi-hop data collection protocol built atop of TeenyLIME was applied to improve the system's flexibility and scalability. The system has been operating since September 2008. After a period of debugging and adjustment, it now acquires data continuously with little or no interruption. In the last 5 months, the data loss ratio was estimated as less than 0.01%, which is good performance if compared with other long term wireless sensor systems deployed.

The data acquired so far are in agreement with the prediction estimated a priori from the 3-dimensional FEM. In particular, the effect of temperature on the deformation of the tower is in line with the estimate; we demonstrated the ability of the system to handle temperature effects, and to calculate compensated deformation records using a Bayesian algorithm. A Bayesian updating procedure is also employed to real-time estimate the probability of abnormal condition states. The proposed Bayesian identification procedure provides a good tool evaluating not only the occurrence of anomalous situations, but also the degree of confidence in this information. In the example reported, the system calculates that the probability of a trend in deformation is, based on the data available, close to zero. In general, the data recorded to date, both from the accelerometer and the deformation sensors, do not raise any special concern as to the safety of the tower. Nevertheless this first period of operation demonstrated the stability and reliability of the system, and therefore its ability to recognize any possible occurrence of an abnormal condition that could jeopardize the integrity of the frescos.

## Acknowledgements

coauthors. Many others contributed to the development and success of this work: specifically, the authors wish to thank: Luca De Bonetti, Alessandro Coppola, Matteo Appollonia, Massimo Cadrobbi, Giorgio Fontana, Giovanni Soncini.

## References

Arms, S.W., Townsend, C.P., Churchill, D.L., Galbreath, J.H., Corneau, B., Ketcham, R.P. and Phan, N. (2008), "Energy harvesting, wireless, structural health monitoring and reporting system", *Proceedings of the 2nd AsiaPacific Workshop on SHM*, Melbourne, December.

Bastianini, F., Matta, F., Rizzo, A., Galati, N. and Nanni, A. (2006), "Overview of recent bridge monitoring applications using distributed brillouin fiber optic sensors", *Proceedings of the 7th Structural Materials Technology (SMT): NDE/NDT for Highways and Bridges and the 6th International Symposium on NDT in Civil Engineering (NDT-CE)*, (Ed. I. Al-Qadi and G. Washer), August.

Bennett, R., Hayes-Gill, B., Crowe, J.A., Armitage, R., Rodgers, D. and Hendroff, A. (1999), "Wireless Monitoring of Highways", *Proceedings of the Smart Structures and Materials 1999: Smart Systems for Bridges, Structures, and Highways*, Newport Beach, CA, USA, March.

Beck, J.L. and Katafygiotis, L.S. (1998), "Updating models and their uncertainties, I: Bayesian statistical framework", *J. Eng. Mech.-ASCE*, **124**(2), 455-461.

Beck, J.L. and Au, S.K. (2002), "Bayesian Updating of Structural Models and Reliability using Markov Chain Monte Carlo Simulation", *J. Eng. Mech.-ASCE*, **128**(4), 380-391.

British Standards Institution (BSI) (1993), *BS 7385-2 Evaluation and measurement for vibration in buildings. Guide to damage levels from groundborne vibration*, BSI, London, UK.

Caffrey, J., Govindan, R., Johnson, E.A., Krishnamachari, B., Masri, S., Sukhatme, G., Chintalapudi, K., Dantu, K., Rangwala, S., Sridharan, A., Xu, N. and Zuniga, M. (2004), "Networked Sensing for Structural Health Monitoring", *Proceedings of the 4th International Workshop on Structural Control*, Columbia University, New York, June.

Casas, J.R. and Cruz. P.J.S. (2003), "Fiber optic sensors for bridge monitoring", *J. Bridge Eng.- ASCE*, **8**(6), 362-373.

Castelnuovo, E. (1987), *Il ciclo dei Mesi di Torre Aquila a Trento*. Museo Provinciale d'Arte, Trento, Italy.

Ceriotti, M., Mottola, L., Picco, G.P., Murphy, A.L., Guna, S., Corrà, M., Pozzi, M., Zonta, D. and Zanon, P. (2009), "Monitoring heritage buildings with wireless sensor networks: the Torre Aquila deployment", *Proceedings of the 8th ACM/IEEE International Conference on Information Processing in Sensor Networks*, San Francisco, April.

Clayton, E.H., Qian, Y., Orjih, O., Dyke, S.J., Mita, A. and Lu, C. (2006), "Off-the-shelf modal analysis: structural health monitoring with motes", *Proceedings of the International Modal Analysis Conference*, January.

Costa, P., Mottola, L., Murphy, A.L. and Picco, G.P. (2007), "Programming wireless sensor networks with the TeenyLIME middleware", *Proceedings of the 8th ACM/IFIP/USENIX International Middleware Conference*, Newport Beach, CA, USA, November.

D'Ayala, D. and Fodde, E. (eds.) (2008), *Structural Analysis of Historical Constructions: Preserving Safety and Significance,* Balkema, Rotterdam, The Netherland.

Deutsches Institut für Normung e. V. (DIN). (1999), *DIN 4150-3 Erschütterungen im Bauwesen - Teil 3: Einwirkungen auf bauliche Anlage*, DIN, Berlin, Germany.

Farrar, C.R. and Worden, K. (2007), "An introduction to structural health monitoring", *Phil. Trans. R. Soc. A*, **365**(1851), 303-315.

Ganeriwal, S., Kumar, R. and Srivastava, M.B. (2003), "Timing-sync protocol for sensor networks", *Proceedings of the 1st International Conference on Embedded Networked Sensor Systems (SENSYS)*.

Glišiæ, B. and Inaudi, D. (2007), *Fibre Optic Methods for Structural Health Monitoring*. Wiley, Hoboken, NJ.

Inaudi, D. (2005), "Overview of fibre optic sensing to structural health monitoring applications", *Proceedings of the International Symposium on Innovation & Sustainability of Structures in Civil Engineering*, Nanjing, China

Inaudi, D. and Glišiæ, B. (2008), "Overview of fibre optic sensing applications to structural health monitoring", *Proceedings of the Symposium on Geodesy for Geotechnical and Structural Engineering*, Lisbon.

Kijewski-Correa, T., Haenggi, M. and Antsaklis, P. (2005), "Multi-scale wireless sensor networks for structural health monitoring", *Proceedings of the SHM*-II'05, November.

Kim, S., Pakzad, S., Culler, D., Demmel, J., Fenves, G., Glaser, S. and Turon, M. (2007), "Health monitoring of civil infrastructures using wireless sensor networks", *Proceedings of the IPSN'07*, Cambridge, Massachusetts, USA, April.

Kurata, N., Spencer, Jr., B.F. and Ruiz-Sandoval, M. (2005), "Risk monitoring of buildings with wireless sensor networks", *Struct. Control Health Monit*, **12**, 315–327.

Lee, B. (2003), "Review of the present status of optical fiber sensors", *Opt. Fiber Technol.* **9**, 57-79.

Lemke, J. (2000), "A remote vibration monitoring system using wireless internet data transfer", *Proceedings SPIE, International Society for Optical Engineering*, **3995**, 436-445.

Lewis, F.L. (2004), *Wireless sensor networks*, Smart Environments: Technologies, Protocols, and Applications D.J. Cook and S.K. Das, Wiley, Hoboken, NJ.

Lynch, J.P. and Loh, K.J. (2006), "A summary review of wireless sensors and sensor networks for structural health monitoring", S*hock Vib. Digest*, **38**(2), 91-128.

Lynch, J.P., Law, K.H., Kiremidjian, A.S., Kenny, T.W., Carryer, E. and Partridge, A. (2001), "The design of a wireless sensing unit for structural health monitoring", *Proceedings of the 3rd International Workshop on Structural Health Monitoring*, Stanford, CA, September.

Lynch, J.P., Kiremidjian, A.S., Law, K.H., Kenny, T.W. and Carryer, E. (2002a), "Issues in wireless structural damage monitoring technologies", *Proceedings of the Third World Conference on Structural Control*, **2**, 667-672.

Lynch, J.P., Law, K.H., Kiremidjian, A.S., Kenny, T.W. and Carryer, E. (2002b), "A wireless modular monitoring system for civil structures", *Proceedings of the 20th International Modal Analysis Conference*, Los Angeles, CA, USA, February.

Measures, R.M. (2001), *Structural monitoring with fiber optic technology*, Academic Press, Canada.

Modena, C., Lourenço, P.B. and Roca, P. (eds.). (2004), *Structural Analysis of Historical Constructions: Possibilities of Numerical and Experimental Techniques*, Balkema, Rotterdam, The Netherlands.

Papadimitriou, C., Beck, J.L. and Katafygiotis, L.S. (1997), "Asymptotic expansion for reliability and moments of uncertain systems", *J. Eng. Mech.-ASCE*, **123**(12), 380-391.

Pines, D.J. and Lovell, P.A. (1998), "Conceptual framework of a remote wireless health monitoring system for large civil structures", *Smart Mater.Struct.*, **7**, 627-636.

Polastre, J., Szewczyk, R. and Culler, D. (2005), "Telos: enabling ultra-low power wireless research", *Proceedings of the 5th International Conference on Information Processing in Sensor Networks (IPSN)*.

Pozzi, M., Zonta, D., Wu, H.Y. and Inaudi, D. (2008), "Development and laboratory validation of in-line multiplexed low-coherence interferometric sensors", *Opt. Fiber Technol.*, **14**, 281-293.

Sazonov, E., Janoyan, K. and Jha, R. (2004), "Wireless intelligent sensor network for autonomous structural health monitoring", *Proceedings of the SPIE on Smart Structures and Materials: Smart Sensor Technology and Measurement Systems*, San Diego, CA, March.

Sivia, D.S. (2006), *Data Analysis: a Bayesian Tutorial*, Oxford University Press, Oxford, UK.

Sohn, H., Farrar, C.R., Hemez, F.M., Czarnecki, J.J., Shunk, D.D., Stinemates, D.W. and Nadler, B.R. (2003), "A review of structural health monitoring literature: 1996-2001", *Los Alamos National Laboratory Report*, LA-13976-MS

Sohn, H. and Law, K.H. (1997), "A bayesian probabilistic approach for structure damage detection", *Earthq. Eng. Struct. D.*, **26**(12), 1259-1281.

Spencer, Jr., B.F., Ruiz-Sandoval, M.E. and Kurata, N. (2003), "Opportunities and challenges for smart sensing technology", *Proceedings of the First International. Conference on Structural Health Monitoring and Intelligent Infrastructure,* Tokyo, November.

Straser, E.G. and Kiremidjian, A.S. (1998), *A Modular, Wireless Damage Monitoring System for Structures*, Technical Report 128, John A. Blume Earthquake Engineering Center, Stanford University, Stanford, CA.

Wu, H.Y. (2009), *Fiber optic sensors and damage evaluation methods for structural health monitoring*, PHD thesis, University of Trento.

Xu, N., Rangwala, S., Chintalapudi, K., Ganesan, D., Broad, A., Govindan, R. and Estrin, D. (2004), "A wireless sensor network for structural monitoring", *Proceedings of the SenSys '04,* Baltimore, Maryland, USA, November.

Zonta, D., Pozzi, M. and Zanon, P. (2008), "Managing the historical heritage using distributed technologies", *Int. J. Architect. Herit.*, **2**, 200-225.

Zonta, D., Pozzi, M., Wu, H.Y. and Inaudi, D. (2009), "Bayesian logic applied to damage assessment of a smart precast concrete element", *Key Eng. Mater.*, **413-414**, 351-358.